Available online at www.sciencedirect.com

ScienceDirect

Current Opinion in Cell Biology

Mapping chemoattractant gradients in live tissues

Boldizsár Vámosi[1,3] and Balázs Enyedi[1,2,3]

Chemoattractant gradients guide cell migration in immunity, tissue repair, and development, yet their spatial and temporal distribution remains difficult to measure. In this review, we discuss how the field is moving beyond static source maps and indirect cellular proxies toward direct visualization of extracellular guidance cues. We outline the strengths and limitations of classical approaches for inferring chemoattractant gradients and highlight new strategies provided by genetically encoded chemoattractant indicators (GECHIs). Emerging PBP- and GPCR-based biosensors enable continuous visualization and localization of extracellular ligands in living tissues using fluorescence intensity- or lifetime-based readouts. Although the current toolbox is limited to a small number of chemoattractants, ongoing sensor development is likely to expand ligand coverage and enable multiplexed measurements with spectrally distinct sensors in the near future.

Addresses
[1] Department of Physiology, Semmelweis University, Faculty of Medicine, Tűzoltó utca 37-47, H-1094, Budapest, Hungary
[2] MTA-SE Lendület Tissue Damage Research Group, Hungarian Academy of Sciences and Semmelweis University, H-1094, Budapest, Hungary
[3] HCEMM-SE Inflammatory Signaling Research Group, Department of Physiology, Semmelweis University, H-1094, Budapest, Hungary

Corresponding author: Enyedi, Balázs (enyedi.balazs@semmelweis.hu)

Current Opinion in Cell Biology 2026, **102**:102676

This review comes from a themed issue on **Cell Dynamics (2026)**

Edited by **Milka Sarris** and **Roop Mallik**

For complete overview of the section, please refer the article collection - Cell Dynamics (2026)

Available online 29 July 2026

https://doi.org/10.1016/j.ceb.2026.102676

Introduction

Chemoattractants drive cell migration in immunity, tissue repair, and development by providing spatial information to guide directed movement and coordinate collective behaviors. Ranging from chemokines to lipid mediators, complement fragments, formyl peptides, and nucleotides, chemoattractants are interpreted primarily through G protein-coupled receptors [1–3]. Once released, they form dynamic extracellular gradients shaped by diffusion and convection, reversible binding to matrix and cell-surface glycans, proteolytic and chemical modifications and scavenging by receptors on neighbouring cells [4,5]. As a result, chemoattractant distributions that migrating cells experience can change within minutes and over distances of a few microns, requiring fast navigational decisions by highly motile cells such as leukocytes [6].

Despite decades of work defining chemoattractant sources, receptors, and downstream signaling pathways, the spatial distribution of functionally available chemoattractants in tissues remains poorly resolved. Historically, chemoattractant distributions have been inferred indirectly from bulk biochemical measurements on homogenized samples, fixed-tissue localization by immunostaining or *in situ* hybridization, and cell-based readouts of receptor activation, intracellular signaling, or migratory behavior (Figure 1). These approaches have been highly informative, but each sacrifices some combination of spatial resolution, temporal resolution, or direct access to extracellular ligand availability (see Table 1).

In this review, we first trace how methodological advances have shifted the field from mapping chemoattractant sources to probing functional extracellular guidance fields in living tissues. We first examine this progression in three chemokine systems: CXCL12 in development, CCR7 ligands in dendritic cell navigation, and CXCL8-family chemokines in neutrophil recruitment, where increasingly direct measurements have refined mechanistic models of guidance. We then extend this discussion beyond chemokines, focusing mainly on leukocyte migration. We consider direct and indirect strategies for measuring or inferring gradients of small-molecule chemoattractants and damage signals, including LTB_4, fMLF, nucleotides, and H_2O_2. Finally, we discuss the emerging class of genetically encoded chemoattractant indicators (GECHIs) including PBP- and GPCR-based biosensors that enable continuous *in situ* reporting of extracellular chemoattractant availability together with the limitations that will shape their broader use.

Figure 1

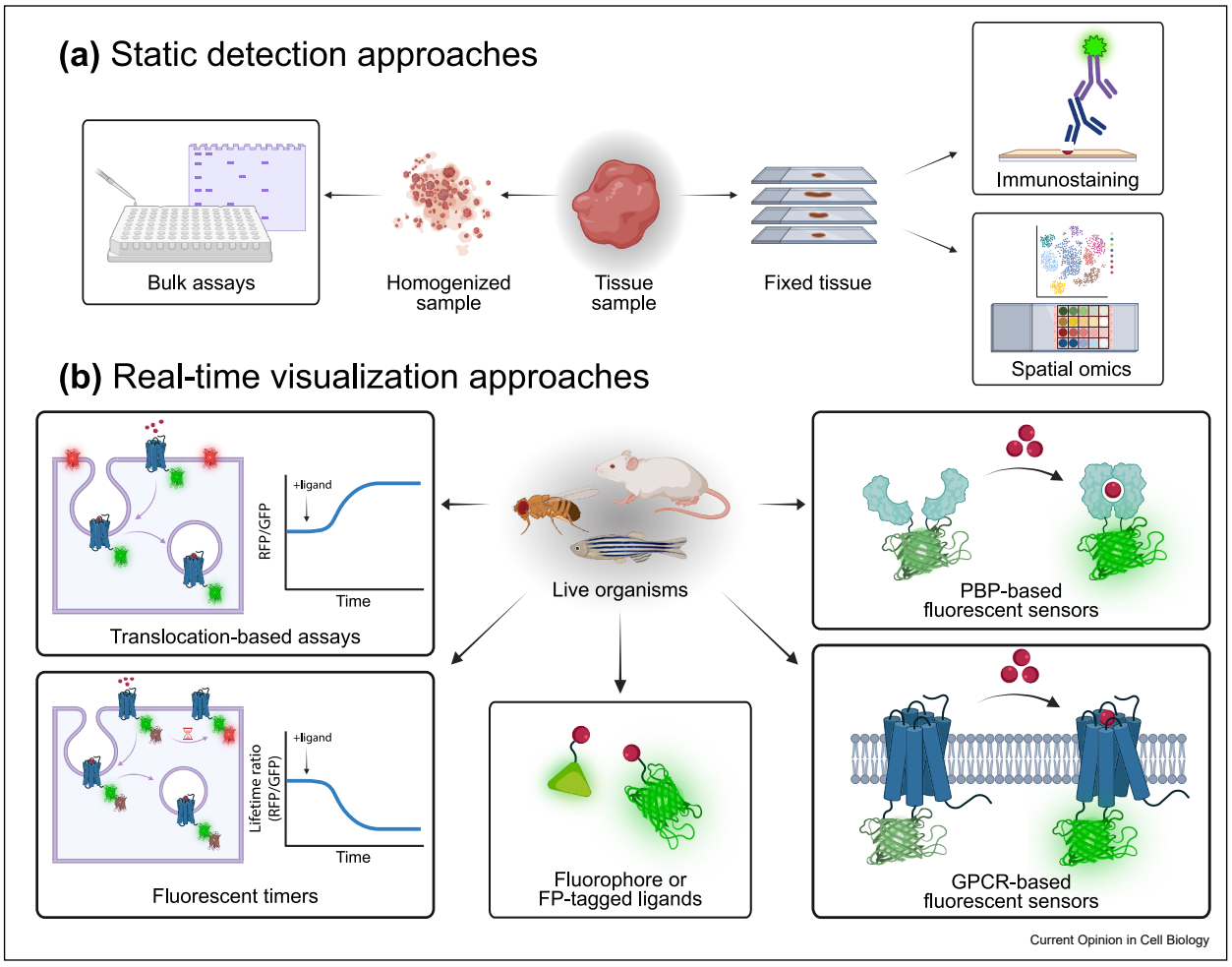

Methods for detecting chemoattractants. **(a)** Bulk assays such as ELISA and Western blotting provide highly sensitive and quantitative measurements, while fixed-tissue approaches reveal detailed maps of chemoattractant distribution. However, these methods rely on endpoint sampling and tissue homogenization or fixation, resulting in poor temporal resolution and in the case of bulk assays, near-complete loss of spatial information. **(b)** Fluorophore- or fluorescent protein-tagged ligands, receptor translocation-based assays, and fluorescent timers enable continuous monitoring of the functionally available ligand pool. However, fluorescent tagging is restricted to ligands that tolerate these modifications, and receptor turnover-based approaches are limited to ligand–receptor pairs in which ligand binding drives robust receptor internalization. These readouts also reflect temporally integrated ligand exposure, limiting temporal resolution. By contrast, PBP- and GPCR-based genetically encoded fluorescent indicators directly report ligand abundance by coupling binding-induced conformational changes to alterations in fluorescence properties, enabling direct and continuous visualization of chemoattractant gradients *in vivo* at unprecedented spatiotemporal resolution.

Classic methods to study chemoattractant guidance and gradient distribution

Studies of primordial germ cells, dendritic cells (DCs), and neutrophils illustrate how successive advances in measuring and interpreting chemoattractant gradients have refined mechanistic models of cell migration and tissue-level ligand distribution.

Visualization of chemokines by fixed-tissue localization

Early efforts to map chemokine expression and distribution relied on *in situ* hybridization and immunostaining to identify producing cells, define tissue localization patterns, and infer how these patterns guide the migration of responsive cells. Such approaches established, for example, the "stripe" of *cxcl12a* expression along the migratory path of the zebrafish posterior lateral line, identified CXCL12-enriched niches in adult hematopoietic tissues, and later revealed CXCL12-containing neutrophil trails associated with the guidance of T cells in influenza-infected airways [7–10]. At the same time, they could not explain how observed chemokine localization patterns are converted into the dynamic directional information perceived by migrating cells in living tissues.

Table 1

Details of approaches described in Figure 1.

Approach	Readout	Directness	Spatial resolution	Temporal resolution	Key caveats/considerations
Bulk assays	Total ligand abundance	+	–	Endpoint	No spatiotemporal sampling; not applicable *in vivo*.
Fixed-tissue localization	Retained distribution of ligand	+	+++	Endpoint	Preserves tissue architecture but may not accurately capture soluble/mobile ligand pools.
Fluorescent ligand	Tagged ligand distribution	++	++	Real-time	Tagging may alter receptor binding, diffusion, matrix interactions and processing.
Receptor internalization/timers	Exposure history	++	+++	Integrated	Reports ligand perception rather than ligand concentration; influenced by receptor trafficking, desensitization, and degradation.
GECHIs	Ligand occupancy	+++	+++	Real-time	Potential ligand buffering, residual signaling, and receptor promiscuity based on sensor design. Reports occupancy rather than absolute concentration.

CCR7 ligand distribution has likewise been studied extensively by *in situ* hybridization and immunostaining [11–15]. In the lymphatic system, these approaches showed that ACKR4-dependent scavenging helps establish properly oriented CCL21 gradients that guide DC migration in lymph nodes [14]. Quantitative immunostaining in mouse skin resolved steep perilymphatic CCL21 gradients linked to how DCs approach lymphatic vessels, providing *in vivo* support for haptotaxis [16]. Subsequent work further showed that the interstitial CCL21 gradient shape is independent of heparan sulfates produced by lymphatic endothelium and can be dynamically remodeled by proteolytic cleavage that increases ligand solubility [17,18]. While these static maps were well suited for the visualization of surface-immobilized CCL21, the extent to which freely diffusible chemokines, including non-immobilized CCL19 and soluble CCL21 species are preserved during fixation and staining remains uncertain, raising the possibility that conventional immunostaining underestimates this mobile pool.

Live imaging of labeled chemokines and receptors

A major conceptual advance was to use ligand–receptor interactions as dynamic reporters of extracellular chemokine availability. In migrating zebrafish primordial germ cells, expression of Cxcr4b–EGFP enabled direct visualization of receptor redistribution and ligand-triggered internalization *in vivo*, demonstrating that receptor trafficking can serve as an optical proxy for local chemokine exposure [19]. In the zebrafish lateral line, pairing a Cxcl12a–GFP ligand reporter with a ratiometric Cxcr4b internalization readout (Cxcr4b–Kate2 together with a membrane marker) separated total ligand abundance from the signaling-competent pool inferred from receptor engagement, revealing a graded signaling landscape despite near-uniform total Cxcl12a levels along the stripe [20]. These measurements converged on a model in which the lateral line creates and maintains a self-generated gradient, with ACKR3-dependent scavenging at the rear shaping gradient steepness and feedback helping to keep ligand availability within a range compatible with robust directional migration [20–22].

A tandem fluorescent timer (tFT) strategy provided complementary support for this model [23]. In this approach, Cxcr4b was fused to a fast-maturing superfolder GFP (sfGFP) and a slower-maturing TagRFP. Chemokine-driven internalization shifts the receptor population toward younger molecules, lowering the red/green 'lifetime' ratio and thereby providing an *in vivo* proxy for local CXCL12 activity. This approach was instrumental in showing that the primordium sculpts a

self-generated CXCL12a activity gradient, one of the first direct *in vivo* demonstrations of gradient shaping by receptor-mediated ligand uptake [24].

Using labeled chemokines also advanced our understanding of CCR7-dependent DC guidance and transmigration across the lymphatic endothelium: CCL21-mCherry was used to identify a chemokine-mediated feedback loop between DCs and lymphatic endothelial cells, in which DCs trigger chemokine release at endothelial junctions [17]. Fluorescent CCL19 and CCL21 variants further expanded this toolkit by enabling real-time analysis of ligand binding, uptake, and redistribution in systems that distinguish CCR7-dependent capture from ACKR4-mediated scavenging, a key mechanism shaping chemokine availability in lymphoid microenvironments [14,25].

The role of strong heparan sulfate proteoglycan binding in shaping the tissue distribution and neutrophil-guiding activity of CXCL8 has also been a long-standing question [26,27]. Zebrafish imaging has been pivotal in addressing this *in vivo*: by creating a controlled focal source of xenografted cells secreting zCxcl8—mCherry, Sarris and colleagues visualized a short-range tissue-bound chemokine gradient and quantitatively linked it to neutrophil migration toward the source [28]. More recently, further zebrafish work demonstrated that differential ligand-induced trafficking of the two zCxcl8 receptors, Cxcr1 and Cxcr2, is sufficient to orchestrate neutrophil clustering and dispersal at sites of tissue damage [29]. Neutrophil-specific Cxcr1/Cxcr2 fluorescent timers provided quantitative, *in vivo* readouts of receptor turnover and exposure history, shifting the perspective from CXCL8 as a simple attractant to a model in which immobilized chemokine gradients and receptor dynamics jointly shape recruitment, retention, and resolution. At the same time, where the signaling-competent CXCL8 pool resides over time, how it equilibrates with GAG-bound interstitial and vascular reservoirs, and how these gradients are sculpted remain open questions that call for tools capable of directly measuring extracellular CXCL8 availability in living tissues.

A key distinction between these approaches is whether they report ligand distribution itself or the cellular response to ligand exposure. Fluorescently tagged ligands report the distribution and potential cellular uptake of the ligand, if native diffusion, receptor-binding, and signaling properties are preserved. Receptor redistribution, internalization, and fluorescent-timer strategies instead infer the exposure history of a ligand-sensing cell, integrating receptor engagement, adaptation, desensitization, recycling, and ligand uptake. The latter can be highly informative because it reflects the signal perceived by the cell, but the relationship to extracellular ligand concentration can be indirect and temporally filtered.

Measuring gradients of small-molecular inflammatory cues

In addition to chemokines, leukocyte navigation is guided by rapidly generated gradients of small molecules that act as early "danger" signals, amplification cues, and drivers of resolution. In zebrafish wounds, H_2O_2 was directly visualized using the biosensor HyPer as an immediate, tissue-scale gradient emanating from the injury margin and functioning upstream of neutrophil recruitment [30]. Subsequent work linked H_2O_2 production to downstream lipid peroxidation and the generation of bona-fide chemoattractant lipids to illustrate how short-lived metabolites in a tissue can serve as directional information after damage [31,32].

Work in mammalian sterile injury further established that formyl peptides, such as fMLF - classically associated with microbial sensing - can also function as potent chemotactic cues in damaged tissues and contribute, together with ATP released from necrotic cells, to early neutrophil guidance [33]. Alongside these early cues, neutrophil-derived lipid mediators create self-amplifying inflammatory gradients: leukotriene B_4 (LTB_4) is well established as a relay signal that recruits additional neutrophils and is central to collective behaviors such as swarming [34—37]. Conversely, lipid signals can also impose negative control: PGE_2 and LXA_4 have been implicated in shaping neutrophil dynamics during inflammation and promoting resolution [38,39].

Despite their established role, precise measurement of the molecules above remains a common challenge. Unlike transcriptionally encoded chemoattractants, small-molecule cues are produced, modified, and cleared on even faster timescales and likely shorter distances, making their *in situ* distributions difficult to infer from endpoint assays. Direct labeling or immunofluorescent detection therefore remains limited, and although emerging spatial metabolomic and mass spectrometry imaging approaches may eventually allow detection at single-cell scale, these methods mainly remain restricted to fixed or cryosectioned tissue samples (Figure 2a) [40,41].

Chemical indicators can be useful to detect small-molecule guidance cues under certain conditions: small-molecule ROS probes and Ca^{2+} dyes have provided important readouts of tissue oxidation, cellular

Figure 2

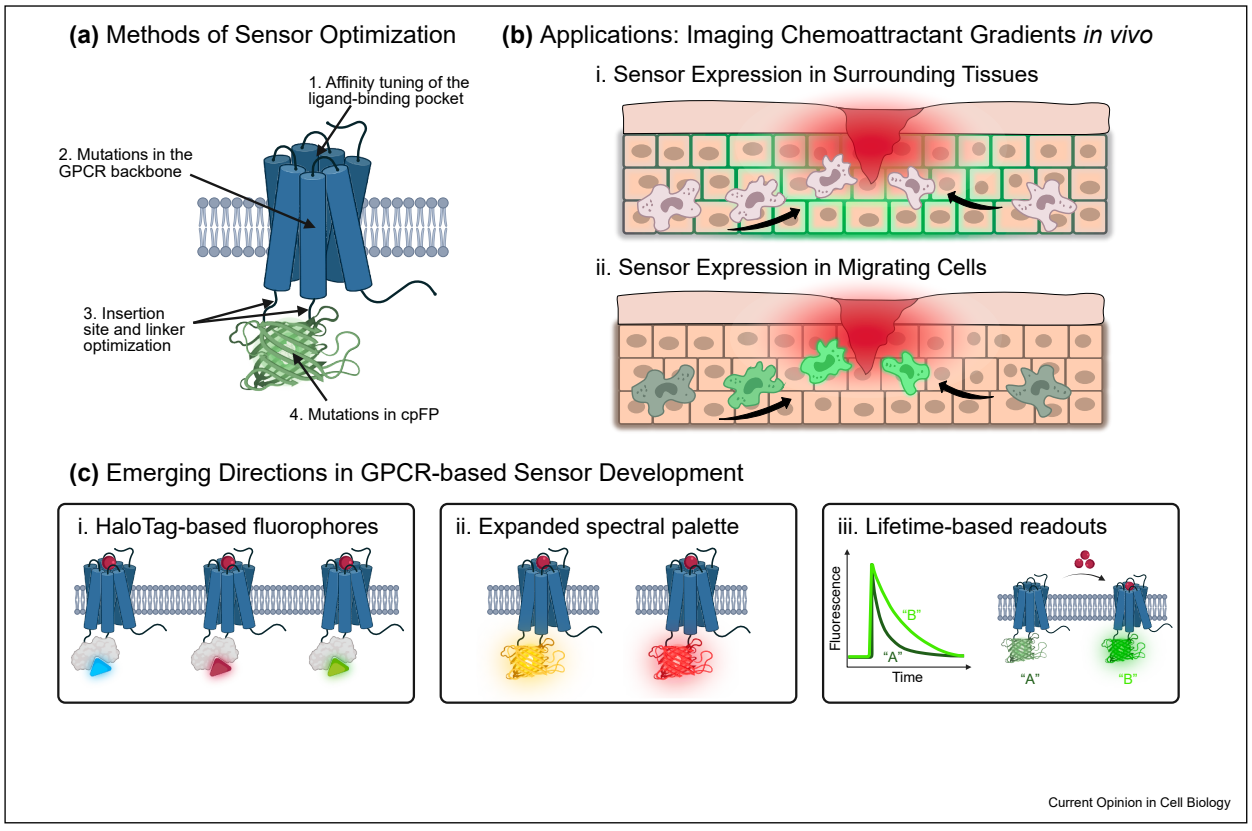

Present and future of GPCR-based fluorescent sensors. **(a)** Development of GPCR-based fluorescent sensors typically requires extensive optimization and therefore requires high-throughput screening strategies. Ligand affinity can be tuned by rational mutagenesis of the binding pocket, and iterative refinement of the GPCR backbone, cpFP insertion site, linker length and composition, along with mutations of the fluorescent protein can influence affinity, dynamic range, basal fluorescence, and downstream signaling properties of the sensor. **(b)** Since these sensors are genetically encoded, they can be expressed in a cell type-specific manner, enabling chemoattractant gradients to be mapped either (i) within surrounding tissues or (ii) in the cells responding to the gradient. **(c)** Advances in both sensor engineering and optical readout strategies are broadening the applicability of GPCR-based sensors. (i) Orthogonal labeling approaches and (ii) an expanding palette of cpFPs are making multiplexed imaging of parallel processes increasingly feasible. In addition, (iii) moving from intensiometric to fluorescence lifetime-based readouts may reduce measurement bias from variable probe expression levels and excitation laser intensity.

activation, and chemoattractant-induced signaling dynamics. However, many ROS indicators report changes in cellular redox state or cumulative oxidative chemistry rather than a single molecular species: for example, DCF-based probes are not specific for H_2O_2 and require careful interpretation [42]. Boronate-based probes provide a more selective chemical strategy, but they also require specificity controls as they may react with other oxidants such as peroxynitrite or hypochlorous acid and can have limited sensitivity for physiological H_2O_2 levels [42]. Ca^{2+} imaging provides a powerful functional proxy for chemoattractant exposure and signal propagation, as illustrated by recent work linking neutrophil swarming to multicellular Ca^{2+} waves, but it reports downstream cell activation rather than extracellular ligand concentration [37,43]. Similar considerations apply to extracellular ATP measurements, where luciferin–luciferase assays and related approaches can sensitively detect nucleotide release but usually lack the spatial or cellular resolution needed to reconstruct dynamic tissue gradients [44]. Genetically encoded probes, including HyPer-family H_2O_2 sensors and GCaMP-type Ca^{2+} indicators address several of these limitations by enabling live imaging, targeted expression in defined cells or tissues, and in many cases ratiometric readouts [45,46]. As discussed below, genetically encoded probes for small-molecule cues, such as $GRAB_{ATP1.0}$ and GEM-LTB_4 extend these approaches by enabling direct detection of extracellular chemoattractant availability, as opposed to indirect measurements of downstream cellular responses triggered by receptor activation. Thus, chemical indicators remain valuable for accessible measurements,

especially in primary human cells or systems where genetic manipulation is difficult, but genetically encoded biosensors provide a more flexible route toward cell-type-specific, real-time mapping of rapidly produced small-molecule chemoattractants in living tissues.

A new era: receptor-based genetically encoded fluorescent biosensors

Although direct fluorescent tagging of chemoattractants and their receptors proved invaluable in pioneering *in vivo* studies, these approaches generally do not measure extracellular ligand concentration directly. Instead, they infer ligand exposure from systems in which ligand binding drives robust, quantifiable receptor internalization, or from ligands that tolerate fusion or chemical labeling, such as chemokines. A further limitation is that exogenous receptor expression can buffer ligand availability and perturb endogenous ligand—receptor stoichiometry. In addition, internalization-based readouts depend on endocytosis, recycling, and degradation kinetics, such that they often report a temporally integrated history of exposure, potentially with a lag that filters rapid fluctuations in extracellular ligand levels (Figure 1b).

By contrast, fluorescent protein (FP)-based genetically encoded biosensors are designed so that the detection of a molecular event is coupled directly to a change in the fluorescence properties of the reporter. In most cases, a sensing unit, such as a ligand-binding domain undergoes a conformational change that is transduced to a reporting unit, which produces an optical output (Figure 1b) [47]. Depending on design, FP biosensors can generate either ratiometric signals, typically based on FRET, or single-FP intensiometric signals. The sensors often use circularly permuted FPs (cpFPs) having an exposed chromophore environment, which renders them conformationally sensitive [48]. Compared with multi-FP ratiometric designs, single-FP cpFP sensors often achieve larger dynamic ranges, but they are also more susceptible to intensity artifacts caused by motion or focal drift and can be sensitive to environmental variables such as pH or ionic strength [47].

Genetically encoded calcium indicators (GECIs) were among the earliest and most influential sensor families, and the biosensor field has since expanded into a broad toolkit reporting intracellular signaling and biochemical state variables, including ions, metabolites, pH, voltage, and redox state [47,49]. In parallel, efforts to detect extracellular ligands, driven especially by neuroscience, have produced sensor designs well suited to the challenges of chemoattractant mapping, including high spatiotemporal resolution, molecular selectivity in complex tissue environments, and continuous *in situ* readout of ligand availability [50,51].

Design principles of PBP- and GPCR-based biosensors

The emergence of periplasmic binding protein (PBP)- and GPCR-based biosensors has transformed optical detection of neurotransmitters and other extracellular molecules [52]. Both sensor classes exploit ligand-induced conformational change coupled to an FP reporter, but they differ in how they are engineered and which ligand classes they naturally cover [53].

PBPs are soluble bacterial receptors that naturally bind nutrients and small metabolites [54]. Their main advantage as sensor scaffolds is engineerability: through binding-pocket redesign and directed evolution, PBPs can be retuned toward a broad range of small molecules [55]. Ligand-dependent closure can be coupled to changes in fluorescence by inserting the cpFP into the PBP and optimizing linker sequences and further residues of the sensor to efficiently transduce the conformational change to the chromophore environment [56]. In favorable cases this yields large intensiometric responses ($\Delta F/F_0$), as exemplified by the iGluSnFR family [56,57]. Because the scaffold is soluble, PBP-based sensors can also be targeted flexibly to the cytosol, organelles, or the extracellular space through secretion or anchoring strategies. In addition, they are typically less likely than GPCR-based biosensors to perturb endogenous signaling pathways [55].

GPCR-based biosensors take advantage of the fact that many neurotransmitters and chemoattractants already have cognate GPCRs with evolved ligand-binding pockets, providing a natural sensing scaffold that can be converted into a fluorescent reporter of ligand engagement [51]. Structurally, GPCRs are comprised of seven transmembrane helices with three extracellular and three intracellular loops. Ligand binding induces conformational rearrangements that can be translated into fluorescence changes by inserting a cpFP into permissive cytoplasmic regions, most commonly the third intracellular loop (ICL3) [58]. Developing efficient sensors requires extensive optimization to preserve membrane trafficking while maximizing $\Delta F/F_0$ and minimizing residual signaling, so that the sensor functions primarily as an optical reporter rather than an active receptor. In practice, this is largely an empirical, high-throughput process involving screening of insertion sites and linker libraries, often combined with receptor or cpFP mutagenesis, to identify variants with suitable signal-to-noise ratio, on/off kinetics, and affinity (Figure 2a) [51,59].

The growing set of PBP- and GPCR-based genetically encoded neurochemical indicators (GENIs), including the SnFR, GRAB, and Light families, now covers most major small-molecule neurotransmitters. These tools

enable real-time imaging of ACh, glutamate, GABA, norepinephrine, serotonin, dopamine, ATP, and additional neuromodulators with high spatiotemporal resolution and specificity *in vivo* [58,60]. These advances provide a conceptual template for measuring extracellular ligands beyond neurobiology. For example, $GRAB_{ATP1.0}$, originally developed to measure synaptic ATP release, has also been used to visualize ATP patterns after sterile wounding in zebrafish, consistent with ATP acting as a danger signal [61]. Applying this strategy to chemoattractant gradients requires transgenic expression of the sensor in the tissue where ligand release and distribution are to be monitored (Figure 2b).

New insights from genetically encoded chemoattractant indicators

The past few years have seen the emergence of *bona fide* chemoattractant biosensors, GECHIs. A first example was GEM-LTB_4, a BLT1-based green cpEGFP sensor optimized to detect LTB_4 in the low-nanomolar range [62]. In an *ex vivo* assay, stable GEM-LTB_4-expressing HEK293A cells were used as a sensing surface onto which neutrophils were deposited and stimulated with fMLF, enabling direct visualization of radially emanating signals consistent with LTB_4 release from single neutrophils. Endogenous LTB_4 production was also detected in live zebrafish expressing the sensor ubiquitously [62]. A key design requirement for such GPCR-based sensors is minimizing unintended signaling in sensor-expressing cells: in GEM-LTB_4, cpEGFP insertion into ICL3 yields a reporter lacking detectable downstream Ca^{2+} transients and β-arrestin recruitment, consistent with minimal coupling to canonical BLT1 signaling. At the same time, as with other high-affinity GPCR-based sensors, ligand buffering remains an important interpretive caveat at high expression levels [51].

Extending the same engineering logic to chemokines, CRAFi-CCR2 was developed and optimized through high-throughput screening to generate a sensor with large fluorescence responses and nanomolar sensitivity to CCR2 ligands [63]. hCRAFi-CCR2, expressed in cultured primary astrocytes detected temporally resolved chemokine release profiles induced by inflammatory stimulation that closely matched ELISA-quantified concentrations. Long-term imaging of the visual cortex of hCRAFi-CCR2-expressing mice revealed patch-like CCR2 ligand microdomains after systemic LPS challenge and a progressive, injury-centered fluorescence increase following laser ablation [63]. Caveats of the approach are inherent to chemokine biology: because CCR2 is promiscuous, the measured signal reflects a composite of CCR2 ligands rather than the concentration of a single chemokine species.

GRAB-LoX3-1.0 is a further chemokine biosensor, based on CXCR3, that detects its endogenous ligands including CXCL9, CXCL10, and CXCL11 [64]. It exhibits a robust fluorescent response and detects chemokines in the nanomolar sensitivity range. *In vivo*, GRAB-LoX3-1.0 visualized micrometer-scale CXCL10 gradients after skin wounding and helped dissect state-dependent chemokine patterning linked to inflammatory phase transitions [64].

Finally, PBP-based sensors provide a conceptually important contrast, because they can be deployed as purified proteins to directly measure extracellular gradients without genetically modifying the responding cells. Using the aspartate sensor jAspSnFR3 [65], self-generated chemoattractant gradients were visualized during collective bacterial migration, leading to a revision of classic models of bacterial chemotaxis [66].

Concluding remarks and future prospects

GPCR- and PBP-based GECHIs now make it possible to monitor extracellular chemoattractant availability in living systems with a spatiotemporal resolution that was difficult to achieve with previous approaches. By coupling ligand binding directly to fluorescence changes that report ligand availability in real time, these probes move the field beyond endpoint measurements and indirect cellular proxies toward direct measurements of the signals that migrating cells are most likely to sense. Early applications already show that this strategy can reveal chemokine and lipid microdomains *in vivo* [62–64]. As improved sensors and quantitative imaging strategies emerge, these tools should enable direct tests of long-standing models of self-generated gradients, relay signaling, and local buffering and scavenging of chemoattractants.

Multiplexed measurements are also coming into reach (Figure 2c). Although most published chemoattractant reporters are currently GFP-based, the expanding cpFP palette and orthogonal labeling strategies, including HaloTag-based designs, provide realistic routes toward multicolor imaging and integration with readouts such as Ca^{2+} signaling or actin dynamics in the same preparation [67,68].

At the same time, these measurements require careful interpretation. Sensor readouts reflect ligand occupancy rather than absolute concentration, so quantitative comparison depends on normalization and, where possible, calibration across defined ligand concentration ranges in the relevant cellular or tissue context [60]. High sensor expression can also buffer ligand availability and perturb the chemoattractant gradient itself, particularly for GPCR-based sensors, even when downstream coupling and internalization have been strongly reduced. Sensor expression should therefore be minimized or titrated, and where possible, compared with physiological receptor abundance. Receptor promiscuity

remains an additional challenge for inflammatory chemokines and lipid mediators, where a single sensor may integrate several ligands into one optical signal. Sensor-dependent perturbations should be evaluated by testing whether sensor-expressing and non-expressing cells or tissues show comparable migration, signaling, inflammatory recruitment, or ligand clearance. Binding-deficient sensor variants harboring point mutations in the binding pocket provide important controls, and where relevant, signaling-silenced GECHI variants should be developed. Orthogonal measurements such as ELISA, mass spectrometry, pharmacological inhibition, or genetic perturbation of ligand production and degradation can provide useful benchmarks, although they rarely replace calibration in living tissues.

Future progress will therefore depend on both refined probes and more rigorous interpretation. Improved ligand selectivity, expanded spectral diversity, fluorescence lifetime-based readouts, and closer integration with quantitative modeling should enhance both interpretability and multiplexing capacity (Figure 2c) [58,69–71]. As these tools mature, they should allow chemoattractant gradients to be treated less as inferred concepts and more as measurable physical variables that can be linked directly to the rules governing cell navigation *in vivo*.

Author contributions

B.E and B.V wrote and edited the manuscript, B.V prepared the figures.

Declaration of generative AI and AI-assisted technologies in the writing process

During the preparation of this manuscript, the authors used ChatGPT 5.3 to assist with language clarity. Following the use of these tools, the authors thoroughly reviewed and edited the content manually to ensure accuracy and take full responsibility for the final version of the published article.

Declaration of competing interest

The authors declare that they have no known competing financial interests or personal relationships that could have appeared to influence the work reported in this paper.

Acknowledgements

We are grateful to Daniel Legler for his valuable comments on the manuscript. Figures were prepared using BioRender.com. The authors were supported by the National Research, Development and Innovation Office of Hungary under project numbers K 147351, ADVANCED 152292, and 2025-1.2.1-HURIZONT-2025-00025. Additional support was provided by the Thematic Excellence Program of the Ministry for Innovation and Technology of Hungary under project no. TKP2021-EGA-24, by the Momentum grant of the Hungarian Academy of Sciences (LP2018-13/2018), by the János Bolyai Research Scholarship (BO/00659/25), and by the European Union's Horizon 2020 research and innovation program under grant agreement no. 739593 (to B.E.).

Data availability

No data was used for the research described in the article.

References

Papers of particular interest, published within the period of review, have been highlighted as:

* of special interest
** of outstanding interest

1. Metzemaekers M, Gouwy M, Proost P: **Neutrophil chemoattractant receptors in health and disease: double-edged swords**. *Cell Mol Immunol* 2020, **17**:433–450.
2. SenGupta S, Parent CA, Bear JE: **The principles of directed cell migration**. *Nat Rev Mol Cell Biol* 2021, **22**:529–547.
3. Lämmermann T, Kastenmüller W: **Concepts of GPCR-controlled navigation in the immune system**. *Immunol Rev* 2019, **289**:205–231.
4. Majumdar R, Sixt M, Parent CA: **New paradigms in the establishment and maintenance of gradients during directed cell migration**. *Curr Opin Cell Biol* 2014, **30**:33–40.
5. Moore JE, Brook BS, Nibbs RJB: **Chemokine transport dynamics and emerging recognition of their role in immune function**. *Current Opinion in Biomedical Engineering* 2018, **5**:90–95.
6. Sarris M, Sixt M: **Navigating in tissue mazes: chemoattractant interpretation in complex environments**. *Curr Opin Cell Biol* 2015, **36**:93–102.
7. Doitsidou M, Reichman-Fried M, Stebler J, Köprunner M, Dörries J, Meyer D, Esguerra CV, Leung T, Raz E: **Guidance of primordial germ cell migration by the chemokine SDF-1**. *Cell* 2002, **111**:647–659.
8. David NB, Sapède D, Saint-Etienne L, Thisse C, Thisse B, Dambly-Chaudière C, Rosa FM, Ghysen A: **Molecular basis of cell migration in the fish lateral line: role of the chemokine receptor CXCR4 and of its ligand, SDF1**. *Proc Natl Acad Sci USA* 2002, **99**:16297–16302.
9. Lim K, Hyun Y-M, Lambert-Emo K, Capece T, Bae S, Miller R, Topham DJ, Kim M: **Neutrophil trails guide influenza-specific CD8$^+$ T cells in the airways**. *Science* 2015, **349**, aaa4352.
10. Kunz L, Schroeder T: **A 3D tissue-wide digital imaging pipeline for quantitation of secreted molecules shows absence of CXCL12 gradients in bone marrow**. *Cell Stem Cell* 2019, **25**:846–854.e4.
11. Willimann K, Legler DF, Loetscher M, Stuber Roos R, Belen Delgado M, Clark-Lewis I, Baggiolini M, Moser B: **The chemokine SLC is expressed in T cell areas of lymph nodes and mucosal lymphoid tissues and attracts activated T cells via CCR7**. *Eur J Immunol* 1998, **28**:2025–2034.
12. Luther SA, Tang HL, Hyman PL, Farr AG, Cyster JG: **Coexpression of the chemokines ELC and SLC by T zone stromal**

cells and deletion of the ELC gene in the *plt/plt* mouse. *Proc Natl Acad Sci USA* 2000, **97**:12694–12699.

13. Schumann K, Lämmermann T, Bruckner M, Legler DF, Polleux J, Spatz JP, Schuler G, Förster R, Lutz MB, Sorokin L, *et al.*: **Immobilized chemokine fields and soluble chemokine gradients cooperatively shape migration patterns of dendritic cells**. *Immunity* 2010, **32**:703–713.

14. Ulvmar MH, Werth K, Braun A, Kelay P, Hub E, Eller K, Chan L, Lucas B, Novitzky-Basso I, Nakamura K, *et al.*: **The atypical chemokine receptor CCRL1 shapes functional CCL21 gradients in lymph nodes**. *Nat Immunol* 2014, **15**:623–630.

15. Russo E, Teijeira A, Vaahtomeri K, Willrodt A-H, Bloch JS, Nitschké M, Santambrogio L, Kerjaschki D, Sixt M, Halin C: **Intralymphatic CCL21 promotes tissue egress of dendritic cells through afferent lymphatic vessels**. *Cell Rep* 2016, **14**:1723–1734.

16. Weber M, Hauschild R, Schwarz J, Moussion C, de Vries I, Legler DF, Luther SA, Bollenbach T, Sixt M: **Interstitial dendritic cell guidance by haptotactic chemokine gradients**. *Science* 2013, **339**:328–332.

17. Vaahtomeri K, Brown M, Hauschild R, De Vries I, Leithner AF, Mehling M, Kaufmann WA, Sixt M: **Locally triggered release of the chemokine CCL21 promotes dendritic cell transmigration across lymphatic endothelia**. *Cell Rep* 2017, **19**:902–909.

18. Collado-Diaz V, Christakopoulou M-N, Schineis P, Blatter K, Laubender D, Trzebanski S, Thoma M, Gadient Y, Tatliadim H, Gkelis K, *et al.*: **uPA-mediated remodeling of CCL21 gradients regulates lymphatic migration of dendritic cells**. *JCB (J Cell Biol)* 2026, **225**, e202412190.

19. Minina S, Reichman-Fried M, Raz E: **Control of receptor internalization, signaling level, and precise arrival at the target in guided cell migration**. *Curr Biol* 2007, **17**:1164–1172.

20. Venkiteswaran G, Lewellis SW, Wang J, Reynolds E, Nicholson C, Knaut H: **Generation and dynamics of an endogenous, self-generated signaling gradient across a migrating tissue**. *Cell* 2013, **155**:674–687.

21. Boldajipour B, Mahabaleshwar H, Kardash E, Reichman-Fried M, Blaser H, Minina S, Wilson D, Xu Q, Raz E: **Control of chemokine-guided cell migration by ligand sequestration**. *Cell* 2008, **132**:463–473.

22. Lau S, Feitzinger A, Venkiteswaran G, Wang J, Lewellis SW, Koplinski CA, Peterson FC, Volkman BF, Meier-Schellersheim M, Knaut H: **A negative-feedback loop maintains optimal chemokine concentrations for directional cell migration**. *Nat Cell Biol* 2020, **22**:266–273.

23. Khmelinskii A, Keller PJ, Bartosik A, Meurer M, Barry JD, Mardin BR, Kaufmann A, Trautmann S, Wachsmuth M, Pereira G, *et al.*: **Tandem fluorescent protein timers for in vivo analysis of protein dynamics**. *Nat Biotechnol* 2012, **30**:708–714.

24. Donà E, Barry JD, Valentin G, Quirin C, Khmelinskii A, Kunze A, Durdu S, Newton LR, Fernandez-Minan A, Huber W, *et al.*: **Directional tissue migration through a self-generated chemokine gradient**. *Nature* 2013, **503**:285–289.

25. Purvanov V, Matti C, Samson GPB, Kindinger I, Legler DF: **Fluorescently tagged CCL19 and CCL21 to monitor CCR7 and ACKR4 functions**. *Int J Mol Sci* 2018, **19**, 3876.

26. Webb LM, Ehrengruber MU, Clark-Lewis I, Baggiolini M, Rot A: **Binding to heparan sulfate or heparin enhances neutrophil responses to interleukin 8**. *Proc Natl Acad Sci USA* 1993, **90**:7158–7162.

27. Cambier S, Gouwy M, Proost P: **The chemokines CXCL8 and CXCL12: molecular and functional properties, role in disease and efforts towards pharmacological intervention**. *Cell Mol Immunol* 2023, **20**:217–251.

28. Sarris M, Masson J-B, Maurin D, Van der Aa LM, Boudinot P, Lortat-Jacob H, Herbomel P: **Inflammatory chemokines direct and restrict leukocyte migration within live tissues as glycan-bound gradients**. *Curr Biol* 2012, **22**:2375–2382.

29. Coombs C, Georgantzoglou A, Walker HA, Patt J, Merten N, Poplimont H, Busch-Nentwich EM, Williams S, Kotsi C, Kostenis E, *et al.*: **Chemokine receptor trafficking coordinates neutrophil clustering and dispersal at wounds in zebrafish**. *Nat Commun* 2019, **10**, 5166.

30. Niethammer P, Grabher C, Look AT, Mitchison TJ: **A tissue-scale gradient of hydrogen peroxide mediates rapid wound detection in zebrafish**. *Nature* 2009, **459**:996–999.

31. Enyedi B, Kala S, Nikolich-Zugich T, Niethammer P: **Tissue damage detection by osmotic surveillance**. *Nat Cell Biol* 2013, **15**:1123–1130.

32. Katikaneni A, Jelcic M, Gerlach GF, Ma Y, Overholtzer M, Niethammer P: **Lipid peroxidation regulates long-range wound detection through 5-lipoxygenase in zebrafish**. *Nat Cell Biol* 2020, **22**:1049–1055.

33. McDonald B, Pittman K, Menezes GB, Hirota SA, Slaba I, Waterhouse CCM, Beck PL, Muruve DA, Kubes P: **Intravascular danger signals guide neutrophils to sites of sterile inflammation**. *Science* 2010, **330**:362–366.

34. Lämmermann T, Afonso PV, Angermann BR, Wang JM, Kastenmüller W, Parent CA, Germain RN: **Neutrophil swarms require LTB4 and integrins at sites of cell death in vivo**. *Nature* 2013, **498**:371–375.

35. Afonso PV, Janka-Junttila M, Lee YJ, McCann CP, Oliver CM, Aamer KA, Losert W, Cicerone MT, Parent CA: **LTB4 is a signal-relay molecule during neutrophil chemotaxis**. *Dev Cell* 2012, **22**:1079–1091.

36. Reátegui E, Jalali F, Khankhel AH, Wong E, Cho H, Lee J, Serhan CN, Dalli J, Elliott H, Irimia D: **Microscale arrays for the profiling of start and stop signals coordinating human-neutrophil swarming**. *Nat Biomed Eng* 2017, **1**, 94.

37. * Strickland E, Pan D, Godfrey C, Kim JS, Hopke A, Ji W, Degrange M, Villavicencio B, Mansour MK, Zerbe CS, *et al.*: **Self-extinguishing relay waves enable homeostatic control of human neutrophil swarming**. *Dev Cell* 2024, **59**:2659–2671.e4.
This study combines live-cell calcium imaging, quantitative modeling, and human neutrophil swarming assays to show that neutrophil recruitment is coordinated by self-extinguishing LTB_4 relay waves, providing evidence that chemoattractant guidance signals can be actively propagated and dynamically constrained during collective migration.

38. Robertson TF, Huttenlocher A: **Real-time imaging of inflammation and its resolution: it's apparent because it's transparent**. *Immunol Rev* 2022, **306**:258–270.

39. Loynes CA, Lee JA, Robertson AL, Steel MJ, Ellett F, Feng Y, Levy BD, Whyte MKB, Renshaw SA: **PGE2 production at sites of tissue injury promotes an anti-inflammatory neutrophil phenotype and determines the outcome of inflammation resolution in vivo**. *Sci Adv* 2018.

40. Zhang H, Lu KH, Ebbini M, Huang P, Lu H, Li L: **Mass spectrometry imaging for spatially resolved multi-omics molecular mapping**. *npj Imaging* 2024, **2**, 20.

41. * Potthoff A, Schwenzfeier J, Niehaus M, Bessler S, Hoffmann E, Soehnlein O, Höhndorf J, Dreisewerd K, Soltwisch J: **Spatial biology using single-cell mass spectrometry imaging and integrated microscopy**. *Nat Commun* 2025, **16**, 9129.
This study reports state-of-the-art high-resolution spatial lipid/metabolite mapping in fixed tissues.

42. Murphy MP, Bayir H, Belousov V, Chang CJ, Davies KJA, Davies MJ, Dick TP, Finkel T, Forman HJ, Janssen-Heininger Y, *et al.*: **Guidelines for measuring reactive oxygen species and oxidative damage in cells and in vivo**. *Nat Metab* 2022, **4**:651–662.

43. Khazen R, Corre B, Garcia Z, Lemaître F, Bachellier-Bassi S, d'Enfert C, Bousso P: **Spatiotemporal dynamics of calcium signals during neutrophil cluster formation**. *Proc Natl Acad Sci USA* 2022, **119**, e2203855119.

44. Gault WJ, Enyedi B, Niethammer P: **Osmotic surveillance mediates rapid wound closure through nucleotide release**. *JCB (J Cell Biol)* 2014, **207**:767–782.

45. Pak VV, Ezerina D, Lyublinskaya OG, Pedre B, Tyurin-Kuzmin PA, Mishina NM, Thauvin M, Young D, Wahni K, Martínez Gache SA, *et al.*: **Ultrasensitive genetically encoded indicator for hydrogen peroxide identifies roles for the oxidant in cell migration and mitochondrial function**. *Cell Metab* 2020, **31**:642–653.e6.

46. Zhang Y, Rózsa M, Liang Y, Bushey D, Wei Z, Zheng J, Reep D, Broussard GJ, Tsang A, Tsegaye G, *et al.*: **Fast and sensitive GCaMP calcium indicators for imaging neural populations**. *Nature* 2023, **615**:884–891, https://doi.org/10.1038/s41586-023-05828-9.

47. Gest AMM, Sahan AZ, Zhong Y, Lin W, Mehta S, Zhang J: **Molecular spies in action: genetically encoded fluorescent biosensors light up cellular signals**. *Chem Rev* 2024, **124**:12573–12660.

48. Miyawaki A, Niino Y: **Molecular spies for bioimaging—fluorescent protein-based probes**. *Mol Cell* 2015, **58**:632–643.

49. Miyawaki A, Llopis J, Heim R, McCaffery JM, Adams JA, Ikura M, Tsien RY: **Fluorescent indicators for Ca2+based on green fluorescent proteins and calmodulin**. *Nature* 1997, **388**:882–887.

50. Patriarchi T, Cho JR, Merten K, Marley A, Broussard GJ, Liang R, Williams J, Nimmerjahn A, von Zastrow M, Gradinaru V, *et al.*: **Imaging neuromodulators with high spatiotemporal resolution using genetically encoded indicators**. *Nat Protoc* 2019, **14**:3471–3505.

51. * Rohner VL, Lamothe-Molina PJ, Patriarchi T: **Engineering, applications, and future perspectives of GPCR -based genetically encoded fluorescent indicators for neuromodulators**. *J Neurochem* 2024, **168**:163–184.
A focused review of the development of GPCR-based neurotransmitter sensors, covering sensor design principles, *in vivo* delivery methods, modes of applications and limitations.

52. Muir J, Anguiano M, Kim CK: **Neuromodulator and neuropeptide sensors and probes for precise circuit interrogation in vivo**. *Science* 2024, **385**, eadn6671.

53. Sabatini BL, Tian L: **Imaging neurotransmitter and neuromodulator dynamics in vivo with genetically encoded indicators**. *Neuron* 2020, **108**:17–32.

54. Berntsson RP-A, Smits SHJ, Schmitt L, Slotboom D-J, Poolman B: **A structural classification of substrate-binding proteins**. *FEBS (Fed Eur Biochem Soc) Lett* 2010, **584**:2606–2617.

55. Leopold AV, Shcherbakova DM, Verkhusha VV: **Fluorescent biosensors for neurotransmission and neuromodulation: engineering and applications**. *Front Cell Neurosci* 2019, **13**, 474.

56. Marvin JS, Borghuis BG, Tian L, Cichon J, Harnett MT, Akerboom J, Gordus A, Renninger SL, Chen T-W, Bargmann CI, *et al.*: **An optimized fluorescent probe for visualizing glutamate neurotransmission**. *Nat Methods* 2013, **10**:162–170.

57. Aggarwal A, Negrean A, Chen Y, Iyer R, Reep D, Liu A, Palutla A, Xie ME, MacLennan BJ, Hagihara KM, *et al.*: **Glutamate indicators with increased sensitivity and tailored deactivation rates**. *Nat Methods* 2026, **23**:417–425.

58. * Yang Y, Li B, Li Y: **Genetically encoded sensors for the in vivo detection of neurochemical dynamics**. *Annu Rev Anal Chem* 2024, **17**:367–392.
A broad review on genetically encoded neurochemical sensors spanning Ca^{2+}, cAMP reporters and neurotransmitter sensors based on PBP and GPCR scaffolds, with particular emphasis on *in vivo* measurements, quantification, multiplexing, and imaging modalities, including intensity- and lifetime-based readouts.

59. Qian T, Wang H, Xia X, Li Y: **Current and emerging methods for probing neuropeptide transmission**. *Curr Opin Neurobiol* 2023, **81**, 102751.

60. Wang H, Qian T, Zhao Y, Zhuo Y, Wu C, Osakada T, Chen P, Chen Z, Ren H, Yan Y, *et al.*: **A tool kit of highly selective and sensitive genetically encoded neuropeptide sensors**. *Science* 2023, **382**, eabq8173.

61. Wu Z, He K, Chen Y, Li H, Pan S, Li B, Liu T, Xi F, Deng F, Wang H, *et al.*: **A sensitive GRAB sensor for detecting extracellular ATP in vitro and in vivo**. *Neuron* 2022, **110**:770–782.e5.

62. ** Tamás SX, Roux BT, Vámosi B, Dehne FG, Török A, Fazekas L, Enyedi B: **A genetically encoded sensor for visualizing leukotriene B4 gradients in vivo**. *Nat Commun* 2023, **14**, 4610.
This study describes the first GECHI, a sensor for leukotriene B4. The BLT1-based fluorescent reporter, GEM-LTB_4 enables the real-time direct visualization of a lipid chemoattractant in living tissues. Using GEM-LTB_4, the authors visualize neutrophil-derived LTB_4 gradients both *in vivo* and *ex vivo*.

63. ** Xiao X, Wang C, Guo X, Xi F, Qian Q, Liang G, Chen M, Sun X, Szabo B, Jing M, *et al.*: **Genetically encoded biosensor for monitoring spatiotemporal dynamics of CCR2 ligands in culture and in vivo**. *Nat Methods* 2025, **22**:1731–1741.
This study describes hCRAFI-CCR2, a genetically encoded fluorescent indicator for CCR2 ligands, revealing spatially heterogeneous chemokine microdomains and dynamic wound-induced CCR2 ligand signaling *in vivo*.

64. ** Xi F, Wang C, Wang Y, Luan P, Chen Y, Tan L, Shang N, Gao X, Chen D, Guo Q, *et al.*: **Spatiotemporal dynamics of CXCL10 encode contextual immune information revealed by the genetically encoded fluorescent sensor**. *Immunity* 2025, **58**:2320–2335.e9.
The authors describe a CXCR3-based biosensor, GRAB-LoX3-1.0, allowing the visualization of micrometer-scale CXCL9-10-11 gradients *in vivo*, revealing chemokine patterning associated with transitions between inflammatory states.

65. Davidsen K, Marvin JS, Aggarwal A, Brown TA, Sullivan LB: **An engineered biosensor enables dynamic aspartate measurements in living cells**. *eLife* 2024, **12**, RP90024.

66. * Phan TV, Mattingly HH, Vo L, Marvin JS, Looger LL, Emonet T: **Direct measurement of dynamic attractant gradients reveals breakdown of the patlak–keller–segel chemotaxis model**. *Proc Natl Acad Sci USA* 2024, **121**, e2309251121.
By combining microfluidic migration assays with a soluble PBP-based sensor for aspartate, the authors directly quantify the spatiotemporal dynamics of a self-generated chemoattractant field during bacterial migration, leading to a revision of classic models of bacterial chemotaxis.

67. Deo C, Abdelfattah AS, Bhargava HK, Berro AJ, Falco N, Farrants H, Moeyaert B, Chupanova M, Lavis LD, Schreiter ER: **The HaloTag as a general scaffold for far-red tunable chemigenetic indicators**. *Nat Chem Biol* 2021, **17**:718–723.

68. ** Zheng Y, Cai R, Wang K, Zhang J, Zhuo Y, Dong H, Zhang Y, Wang Y, Deng F, Ji E, *et al.*: **In vivo multiplex imaging of dynamic neurochemical networks with designed far-red dopamine sensors**. *Science* 2025, **388**, eadt7705.
First report of a chemigenetic GPCR-based sensor using cpHaloTag as the fluorescent module. HaloDA1.0 extends dopamine imaging into the far-red spectral range and enables multiplexed measurements together with green and red reporters.

69. Becker W: **Fluorescence lifetime imaging – techniques and applications**. *J Microsc* 2012, **247**:119–136.

70. ** Ma P, Chen P, Tilden EI, Aggarwal S, Oldenborg A, Chen Y: **Fast and slow: recording neuromodulator dynamics across both transient and chronic time scales**. *Sci Adv* 2024, **10**, eadi0643.
This study shows that several PBP- and GPCR-based neurotransmitter sensors exhibit measurable fluorescence lifetime changes upon ligand binding, and demonstrates with $GRAB_{ACh3.0}$ that lifetime readout can capture both transient and chronic neuromodulator dynamics independently of expression level and excitation power variability.

71. * Tian L, Roshgadol J, Chouinard J, Majumder S, Scott E, Borges K, Hagihara K, Mancini N, Stevenson T, Kamath T, *et al.*: ***Sensitive dLight for imaging broad-spectrum dopamine events across brain regions***. 2025, https://doi.org/10.21203/rs.3.rs-7313638/v1.
This study introduces next-generation GPCR-based dopamine sensors with substantially improved dynamic range, sensitivity, and *in vivo* performance, with dLight3.8 enabling high-fidelity fluorescence lifetime measurements.